A Modularized Two-Stage Charge Equalizer With Cell Selection Switches for Series-Connected Lithium-Ion Battery String in an HEV

Chol-Ho Kim, *Student Member, IEEE*, Moon-Young Kim, *Student Member, IEEE*, Hong-Sun Park, *Associate Member, IEEE*, and Gun-Woo Moon, *Member, IEEE*

***Abstract*—In lithium-ion battery system for hybrid electric vehicle, charge equalizer is essential to enhance the battery life cycle and safety. However, for a large number of battery cells, a conventional equalizer has the difficulty of individual cell balancing and the implementation size problem as well as the cost. Moreover, it shows high voltage stress of electrical elements in the equalization converter due to the high voltage of battery pack. To improve these drawbacks, this paper proposes a modularized two-stage charge equalizer with cell selection switches. The proposed circuit employs the two-stage dc–dc converter to reduce the voltage stress of equalization converter. Contrary to conventional method, the proposed equalizer can achieve the individual cell balancing only through the cell selection switches. With the two-stage converter and the cell selection switches, the proposed equalizer leads to the great size reduction with lower cost which brings advancement of individual cell balancing in a large number of battery cells. In this paper, a prototype for 88 lithium-ion battery cells is optimally designed and implemented. Experimental results are presented to verify that the proposed equalization method has a good cell balancing performance showing the low voltage stress and small size with the lower cost.**

***Index Terms*—Charge equalizer, hybrid electric vehicle (HEV), lithium-ion battery.**

I. Introduction

MANY countries are taking steps to cut the greenhouse gas emissions. Especially, autoemission standards are getting stricter to follow; furthermore, they will force vehicles to become more fuel efficient. With these demands, an electric vehicle (EV) and a hybrid EV (HEV) have attracted more strong attentions for fuel economy and eco-friendly vehicle by automakers, governments, and customers [1], [2]. Compared to the conventional vehicle, an HEV needs a large number of batteries connected in series for driving electronic motors [3]. These batteries can be recharged energy from wheels during regenerative braking, an energy source that was wasted in the past, and reuse it to propel the vehicle at low speeds or boost extra power required in high acceleration [4], [5]. This repeated charge and discharge can cause the charge imbalance among the battery cells because the batteries have inevitable differences in chemical and electrical characteristics, such as the difference of manufacture, mismatched ambient temperature, and asymmetrical cell degradation with aging [7]–[10]. The charge imbalance will decrease the total storage capacity and the whole life cycle of the battery [9], [10]. Hence, charge equalization for a series-connected battery string is necessary to maintain the storage capacity and extended battery lifetime.

Currently, rechargeable lithium-ion batteries are under the consideration of an HEV application because they have been showing good characteristics such as a high energy density, a high single-cell voltage, and a low self-discharge rate. With these benefits, lithium-ion battery comes into the spotlight to the future of vehicles market [6]. However, the lithium-ion battery requires careful management because of the battery's chemistry that cannot withstand overcharged state due to the high risk of explosion. Furthermore, an undercharged battery cell can reduce life cycle of the battery cell [7]–[9]. Therefore, an individual equalization of the battery charge must be provided to prevent any of single cells from over or undercharged stage.

Charge equalization methods for a series-connected battery string have been presented in [10]–[21] and well summarized in [22]. As shown in Fig. 1, these equalizers can be classified into two categories according to the control types: centralized control and cell control. The centralized control equalizer shows a simple structure and a low cost implementation. However, one of the centralized controls such as switched capacitor method shows the prolonged equalization time caused by a cell-to-cell energy shift [10], [11]. The secondary multiple winding also includes the difficulty of implementing a multiple secondary winding in a single transformer [12], [13]. The cell control equalizer has the merit of good equalization performance compared to the centralized-control-based equalizer [14]–[21]. The resistive current shunt is one of the cell control equalizers [14]. This method is an attractive equalization method due to easy implementation and low cost. However, the energy dissipation and heat problem are critical drawbacks in high power application such

Manuscript received May 4, 2011; revised August 17, 2011, and November 16, 2011; accepted January 5, 2012. Date of current version April 20, 2012. This paper was presented at the IEEE Power Electronics Specialist Conference, 15–19 June, 2008, Island of Rhodes, Greece. Recommended for publication by Associate Editor D. Xu.

C.-H. Kim, M.-Y. Kim, and G.-W. Moon are with the Department of Electrical Engineering, Korea Advanced Institute of Science and Technology, Yuseong-Gu, Daejeon 305-701, Korea (e-mail: railroads@angel.kaist.ac.kr; moonx32@angel.kaist.ac.kr; gwmoon@ee.kaist.ac.kr).

H.-S. Park was with the Department of Electrical Engineering, Korea Advanced Institute of Science and Technology, Yuseong-Gu, Daejeon 305-701, Korea. He is now with Samsung Electro-Mechanics, Suwon, Gyeonggi 443743, Korea (e-mail: hongsun.park@samsung.com).

Color versions of one or more of the figures in this paper are available online at http://ieeexplore.ieee.org.

Digital Object Identifier 10.1109/TPEL.2012.2185248

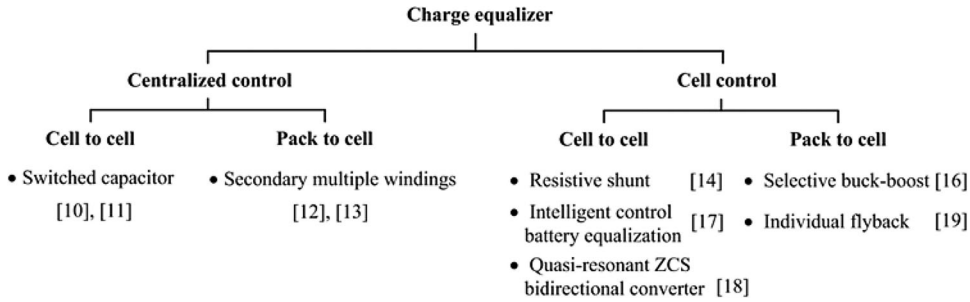

Fig. 1. Classification of conventional battery equalizers.

as an HEV. Other cell control equalizers allocate the separated dc–dc converter to each cell for the individual cell balancing. These methods show high performance of cell balancing and easy control of equalization current; still it has also weak points such as control complexity and implementation cost [15]–[21].

Based on the fact that more than 50 batteries are stacked in series for an HEV, each control category can be divided into two parts according to energy transfer type: cell to cell and pack to cell. In case of cell to cell, each cell should have an individual converter to transfer the balancing energy from normal cells to unbalanced cell. This type cannot be directly applied to a large number of battery cells due to an implementation size and cost. Hence, it should employ the modularized concept of the battery string such that an additional balancing circuit for modular battery stacks is needed in overall equalization system [19]. Compare to the cell-to-cell type, pack-to-cell equalization type shows effective balancing performance without an additional modular balancing. It transfers the balancing energy from overall battery to unbalanced cell. However, this type has the voltage stress problem of dc–dc converters due to the high voltage of overall battery pack.

To improve these defects, this paper proposes a modularized two-stage charge equalizer. The principle of the proposed work is that the equalization energy from the battery pack moves to the target battery cell through the two-stage dc–dc converters and cell selection switches. The two-stage converters can reduce the voltage stress of the proposed equalizer in spite of the pack-to-cell equalization type. The cell selection switches bring forth the advancement of individual cell balancing despite not to use the dedicated converter per each cell. It simply makes the equalization current path between the dc–dc converter and the unbalanced cell. With this configuration, the size and cost problem of the battery equalizer is effectively solved and the individual equalization performance can be easily satisfied.

In this paper, a prototype of 88 lithium-ion battery cells employing the proposed method is optimally designed and implemented. In addition, compared with the equalizer presented in [16]–[19], reduction of used components and controller simplicity is shown for 88 cells. The experimental results are presented to verify that the proposed method has excellent cell balancing performance showing the low voltage stress and small size with the lower cost.

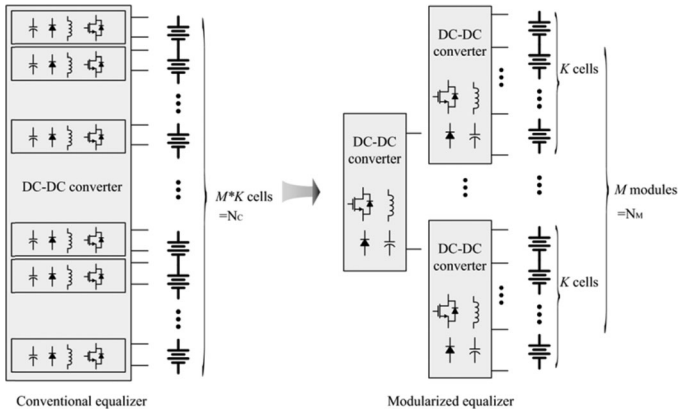

Fig. 2. Modular concept of the proposed equalizer.

II. Proposed Charge Equalizer

The proposed equalizer using the battery modularization is shown in Fig. 2 with comparing to the conventional equalizer. Conventional equalizer is used for one battery string; still proposed equalizer is for divided module unit of battery strings. In the proposed work, let the whole battery string be tied up with the number of M group, which include the number of K cells. In addition, the proposed scheme has the sharing connection of dc–dc converters. One single converter share with multiple module converters; moreover the module converter holds each battery in common. With this modular concept, we can use the electronic device, which has a low voltage stress as well as easy implementation of balancing circuit [23], [24].

Fig. 3 shows the block diagram of the proposed charge equalizer applied to $M*K$ battery cells. The proposed equalizer consists of three parts: the first-stage dc–dc converter, the second-stage dc–dc converter, and selection switch modules. The first-stage converter steps down from high voltage of battery pack to low voltage level. This stage is simply implemented by using the conventional flyback converter. The main work of this stage is to supply equalization power to the second-stage modules. The second-stage converter constructed in each module makes the charging current. The second stage is also implemented by the flyback converter. Lastly, the selection switch module consists of the bidirectional switches to make a current path between

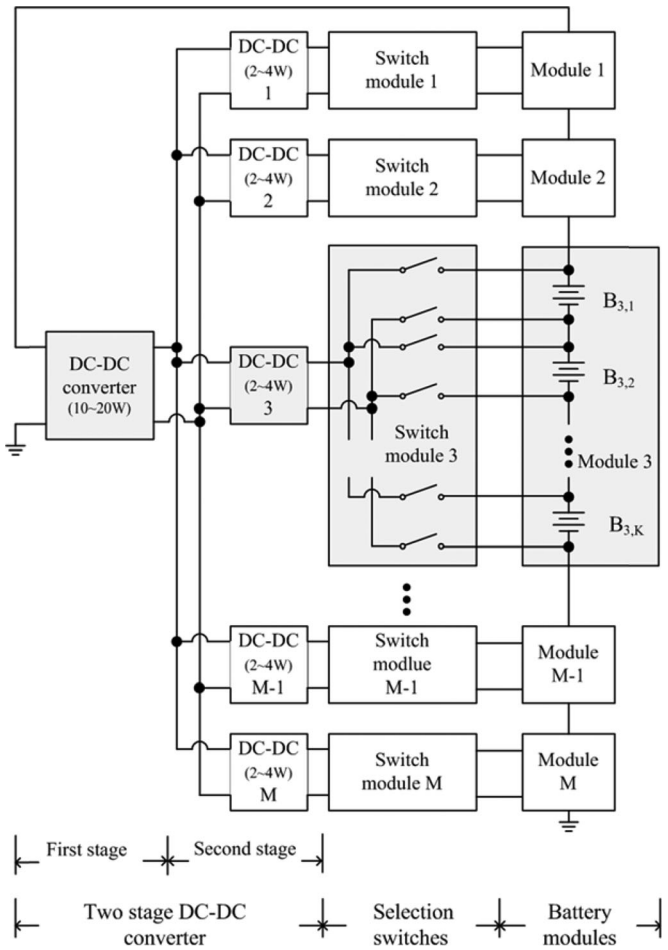

Fig. 3. Block diagram of the proposed two-stage charge equalizer.

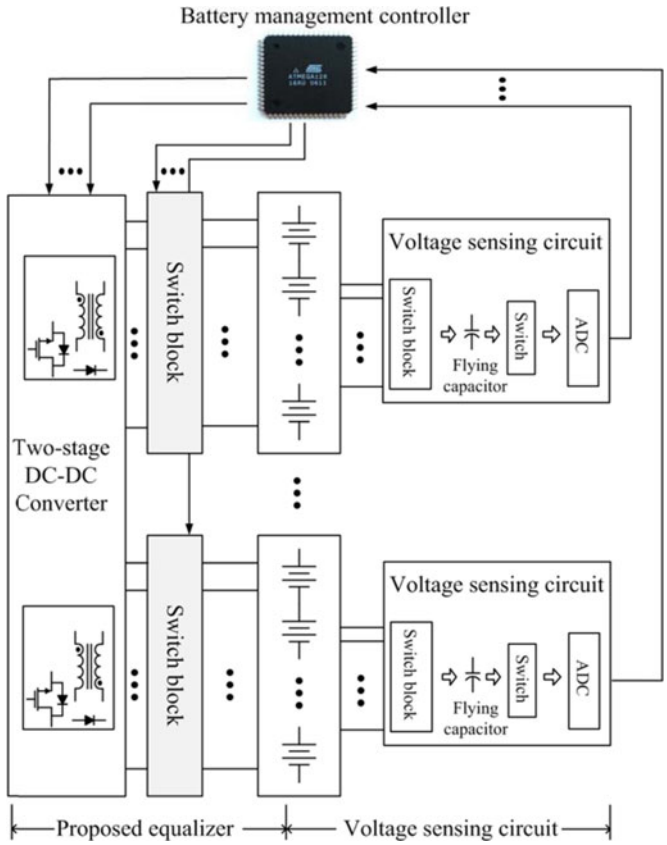

Fig. 4. System configuration of the proposed charge equalizer.

second-stage dc–dc converter and the selected battery cell. The key features of the proposed equalizer are as follows.

1) Easy implementation of the electronic devices can be achieved when a battery string is modularized into plenty of module batteries.
2) In contrast to the allocation of a complete dc–dc converter to each cell [16]–[19], the modular dc–dc converter, which is called as the second-stage converter, is shared by the modularized cells, leads to the great size reduction for the number of dc–dc converters.
3) A common dc–dc converter is connected in parallel with each modular converter, which it can step-down the high voltage from overall battery stack to low voltage with the input voltage of second-stage converter.
4) Similar to the method that is described in [16], individual equalization can be achieve when the cell selection switch can route the equalization current to the lowest voltage cell. In addition, the independent operation process in each module makes the cell balancing more effective.

III. Operational Principles

The proposed charge equalizer transfers the equalization current from the overall battery string into the selected cell. In this process, the battery control system is required to operate each electrical device, such as the cell voltage sensing circuit, the charge equalizer, and battery controller. Fig. 4 shows the system configuration of the proposed equalizer scheme. In this system, the proposed equalizer employs a battery management controller (BMC) with voltage sensing circuitry. The BMC collects the sensing data from the voltage sensing circuit. In the sensing circuit, the cell voltage is transferred into a flying capacitor through a switching block. The BMC reads the voltage of flying capacitor, which is converted by an analog-to-digital converter. After reading the cell voltage, the BMC determines the operation of the charge equalization. Then, it drives the charge equalizer with three consecutive steps.

Before describing these three steps, it is assumed that the second battery of the third module, $B_{3,2}$, is undercharged. Thus, the cell selection switches, $S_{3,2a}$ and $S_{3,2b}$, are turned ON before the operation of the dc–dc converter. In this process, the cell selection switch is kept ON during the cell balancing time. Furthermore, this selection switch is driven with two level signals, such as logical high and logical low signal. The following assumptions are made.

1) The MOSFET switches are ideal except for their internal body diode. Furthermore, the rectifier diodes of the dc–dc converter are ideal.
2) Two-stage dc–dc converters are operated as the ideal current source in steady state.

3) All of the selection switches, $S_{3,2a}$ and $S_{3,2b}$, are modeled as short path when they are turned ON and modeled as open path when they are turned OFF.
4) The six batteries, B_{2,k_3}, B_{2,k_2}, B_{2,k_1}, $B_{3,1}$, $B_{3,2}$, and $B_{3,3}$, each have a constant voltage.

Step 1: When the BMC turns ON the bidirectional switches, $S_{3,2a}$ and $S_{3,2b}$, with BMC command, the first step starts. In this step, the current path for $B_{3,2}$ is constructed. As shown in Fig. 5(a), the charge current can flow into $B_{3,2}$ through this current path.

Step 2: After completely turn-ON of the bidirectional switches, the second-stage dc–dc converter is driven by the BMC. As a result, this second-stage converter is now coupled with $B_{3,2}$, as shown in Fig. 5(b). In this mode, although the second-stage converter operates, the equalization current does not flow into the selected cell. This is because the first stage is not turned ON, such that the second stage has no input power yet.

Step 3: In this mode, the first-stage dc–dc converter is turned ON by the BMC. This stage transfers the equalization current from the battery stack to the input terminal of the second-stage converter. Therefore, by collaborating with the second-stage dc–dc converter and the selection switches, the first-stage converter can provide the equalization current to the undercharged cell, $B_{3,2}$, as shown in Fig. 5(c).

In the proposed circuit, a bidirectional switch for cell selection consists of a pair of MOSFET switches, as shown in Fig. 6(a). These switches should demand simple control and small size to apply to many battery cells. Hence, the MOSFET switches are attractive to adapt the selection switch because it can be easily integrated as small-size component. In this switch structure, there are two kinds of techniques to turn ON the bidirectional switch. As shown in Fig. 6(b), an P-channel MOSFET switch for $B_{1,1}$ can be turned ON by using the optocouplers, $Q_{1,1a}$ and $Q_{1,1b}$. A turn-ON source of the MOSFET comes from the lower layer batteries $B_{1,1}$, $B_{1,2}$, $B_{1,3}$, and $B_{1,4}$. This P-channel MOSFET switches are only used for two cells of the first module, $B_{1,1}$ and $B_{1,2}$. On the other hand, a N-channel MOSFET switch for $B_{1,4}$ can be turned ON by using the optocouplers, $Q_{1,4a}$ and $Q_{1,4b}$, as shown in Fig. 6(c). Its turn-ON source comes from the upper layer batteries, $B_{1,1}$, $B_{1,2}$, $B_{1,3}$, and $B_{1,4}$. With this turn-ON circuit, we can achieve the self-driven procedure for turning ON a MOSFET switches without an auxiliary turn-ON source.

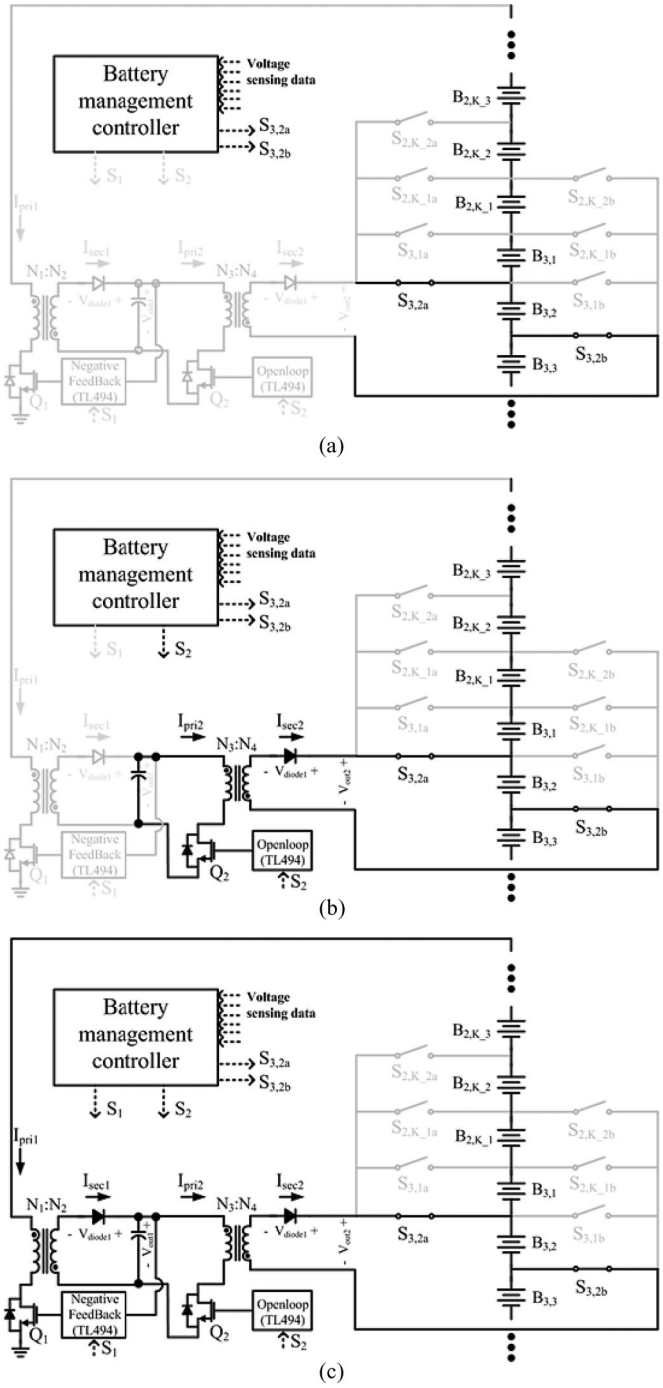

Fig. 5. Operational principles of the proposed circuit. (a) Step 1. (b) Step 2. (c) Step 3.

IV. Design Considerations

A. Optimal Power Rating Design Guide

This section presents the optimal power rating design guide for a charge equalizer. The power rating of an equalization circuit relates closely with the equalization time; again, the higher the power rating, the shorter the equalization time. The power rating is also related with the size of the circuit. Hence, we employ a way of determining the power rating while achieving cell balance within the desired equalization time [19], [20].

Before presenting the power rating design guide, we firstly introduce a modeling of the lithium-ion battery. Fig. 7 shows an example of a battery modeling [19]. In this figure, the open-circuit voltage is plotted according to state of charge (SOC) of a lithium-ion 7 Ah battery. The dot symbol represents the experimental results in range of 10% to 90% according to the SOC. The solid line is the linear approximation of those. The SOC corresponds to the stored battery charge that is available for

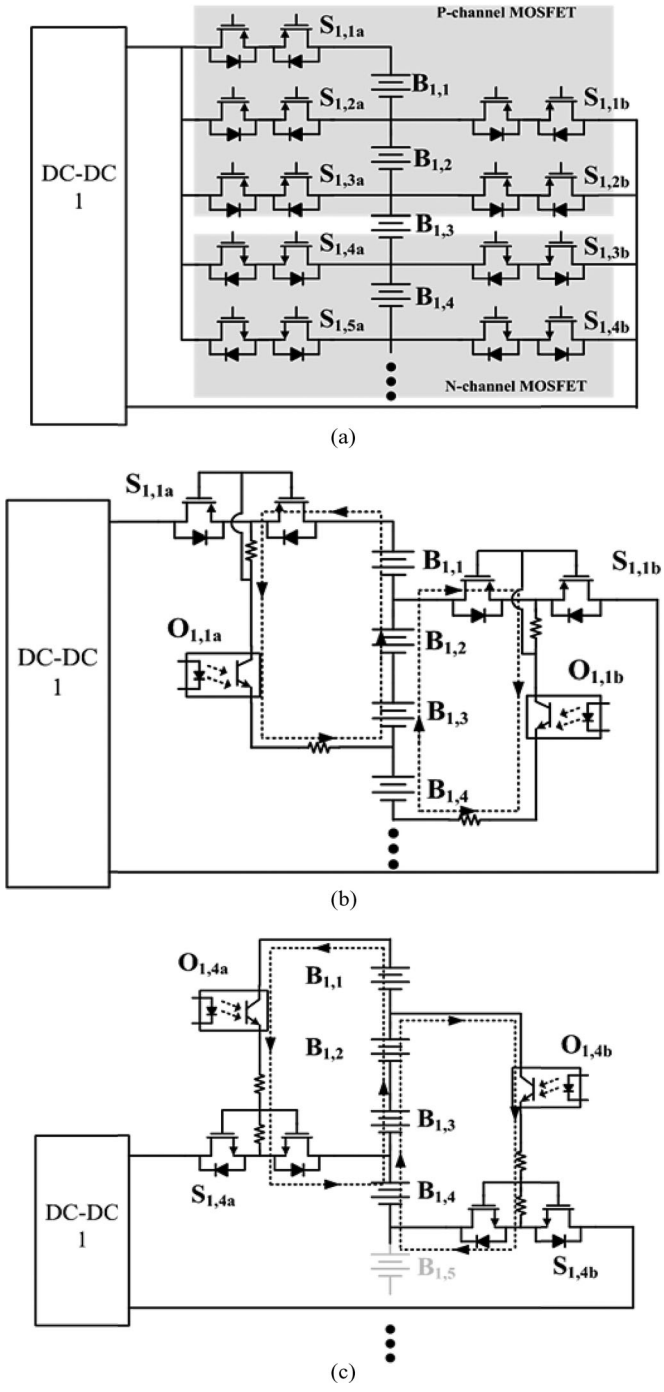

Fig. 6. Cell selection switches base on MOSFET. (a) Structure of cell selection switches. (b) Turn-ON procedure of P-channel MOSFET. (c) Turn-ON procedure of N-channel MOSFET.

doing work, relative to the open-circuit voltage. This modeling is used for the design guide, not appealing to estimate the battery SOC in the proposed work. The battery charge/discharge current control is based on the SOC information [25]–[27].

In power rating design, the following notations are very useful.

1) $Q_n(t)$: charge quantity of the nth cell at time t.

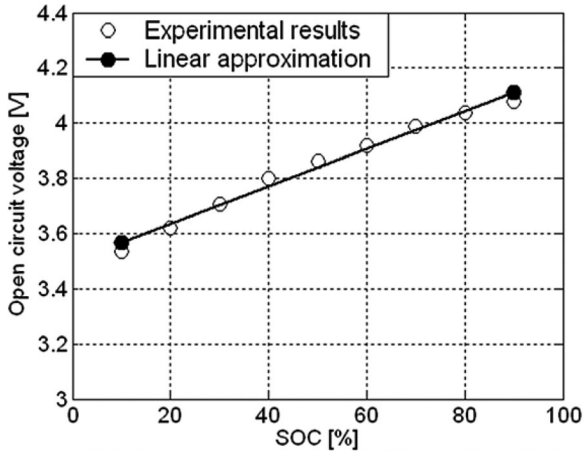

Fig. 7. Linear modeling according to the state of charge for 7 Ah lithium-ion battery.

2) $V_n(t)$: voltage of the nth cell at time t.
3) $I_{\rm in}, I_{\rm out}$: constant input current and output current of the equalizer.
4) I_N: net current between input current and output current $(I_{\rm out} - I_{\rm in})$.
5) $P_{\rm in}(t), P_{\rm out}(t)$: input power and output power of the equalizer at time t.
6) $P_{\rm in,avg}, P_{\rm out,avg}$: average input power and average output power of the equalizer.
7) η: efficiency of a dc–dc converter.

The proposed charge equalizer is applied to the lithium-ion battery string of N cells, where only first cell is assumed to be undercharged. To obtain the optimal power rating for this environment of the battery string, the following simultaneous equations should be satisfied:

$$\frac{1}{N-1}\sum_{n=2}^{N} Q_n(t_{\rm eq}) = Q_1(t_{\rm eq}) \tag{1}$$

$$P_{\rm out,avg} = \eta P_{\rm in,avg} \tag{2}$$

where the left side of (1) is the average charge quantity of the overall batteries except the undercharged cell at equalization time $t_{\rm eq}$, and the right side is the charge quantity of the undercharged battery cell at equalization time $t_{\rm eq}$. Equation (2) indicates the relation between the average input power and the average output power of the proposed converter with efficiency of η. The average input power means the equalization energy which is extracted from the whole battery cells, and the average output power means the equalization energy which flows into the undercharged cell. Furthermore, the amount of average charge remained in the undercharged cell, $Q_1(t)$, and average input and output power of the equalizer, $P_{\rm in,avg}$ and $P_{\rm out,avg}$, are given , respectively, by

$$Q_1(t) = Q_1(0) + I_N t_{\rm eq} = Q_1(0) + (I_{\rm out} - I_{\rm in}) \cdot t_{\rm eq} \tag{3}$$

$$P_{\text{out,avg}} = \frac{1}{t_{\text{eq}}}\int_0^{t_{\text{eq}}} p_{\text{out}}(\tau)d\tau = \frac{1}{t}\int_0^{t} v_1(\tau)I_{\text{out}}d\tau$$
$$= \left(v_1(0) + \frac{1}{2C}(I_{\text{out}} - I_{\text{in}})t_{\text{eq}}\right) I_{\text{out}} \quad (4)$$

$$P_{\text{in,avg}} = \frac{1}{t_{\text{eq}}}\int_0^{t_{\text{eq}}} p_{\text{in}}(\tau)d\tau$$
$$= \frac{1}{t}\int_0^{t} (v_1(\tau) + \sum_{n=2}^{N} v_n(\tau))I_{\text{in}}d\tau$$
$$= \left(\sum_{n=1}^{N} v_n(0) + \frac{1}{2C}(I_{\text{out}} - N\cdot I_{\text{in}})t_{\text{eq}}\right) I_{\text{in}} \quad (5)$$

where C is capacitance of the 7 Ah lithium-ion battery. In this method, the average power is taken into consideration because the cell voltages can change during the equalization time.

By substituting (3)–(5) into (1) and (2), and by solving (1) and (2) jointly, we can obtain the relationship between equalization time t_{eq} and input current I_{in} as follows:

$$t_{\text{eq}} = \frac{C}{I_{\text{in}}}\left(\frac{1}{N}\sum_{n=1}^{N} v_n(0) + \sqrt{\alpha}\right)$$
$$\alpha = \left(\frac{1}{N}\sum_{n=1}^{N} v_n(0)\right)^2 - \frac{1}{\eta N}\left(\left(\frac{1}{N-1}\sum_{n=2}^{N} v_n(0)\right)^2 - (v_1(0))^2\right). \quad (6)$$

From (3) and (6), the relationship between the equalization time and the equalization net current into the undercharged cell I_N can be given by

$$t_{\text{eq}} = \frac{C}{I_N}\left[\left(\frac{1}{N-1}\sum_{n=2}^{N} v_n(0) - v_1(0)\right) - \left(\frac{1}{N}\sum_{n=1}^{N} v_n(0) + \sqrt{\alpha}\right)\right]. \quad (7)$$

With the analysis in the above, the simulation results of the power rating design for 88 cells can be achieved as shown in Fig. 8. In these results, it is assumed that only one cell is undercharged and an SOC difference between the undercharged cell and the other cells is 10%. Moreover, the efficiency of the proposed equalizer is temporarily assumed to be 50%, 60%, and 70%. The equalization time is plotted in relation to the input current of the equalizer and the net current into the undercharged cell. From the simulation results, we know that the shorter equalization time will be taken for the higher input current of equalizer and also the higher net current. In addition, the higher efficiency of equalizer takes the smaller input current. As one design example, to obtain charge balance within 100 min, input current of approximately 0.011 A is required at 50% efficiency. Then, the net equalization current is 0.45 A.

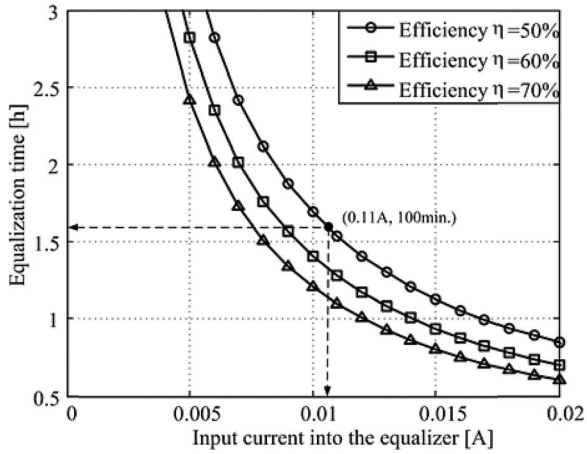

Fig. 8. Simulation results of the optimal power rating design under an SOC difference of 10%. (a) Equalization time versus input current. (b) Equalization time versus net current.

B. Power Circuit Design Guide

Power converter for proposed equalizer requires a reliable circuit designs because input and output power is connected to the lithium-ion battery. Moreover, electrical components for dc–dc converter needs to consider a system size and has enough voltage and current stress margin. As shown in Fig. 9, the proposed equalizer uses a flyback dc–dc converter, which is the simplest circuit among the isolation-type converters. For the proposed system, a flyback converter requires (discrete current mode (DCM) operation. In DCM, current overshoot, switching loss, and RF interference are preferred over continuous current mode (CCM) due to the blocking of the problem of reverse recovery in rectifier diode. A flyback converter with DCM operation can accomplish higher reliability and simplicity of the converter for proposed system.

According to the high input voltage such as HEV battery pack, design consideration of first-stage converter is to obtain the maximum duty ratio $D_{\max}$ for main switch Q_1, under the safety range of voltage stress. The converter guarantees DCM operation at the full-load condition, which is charge equalization with four cells at the same time. In this condition, it is assumed

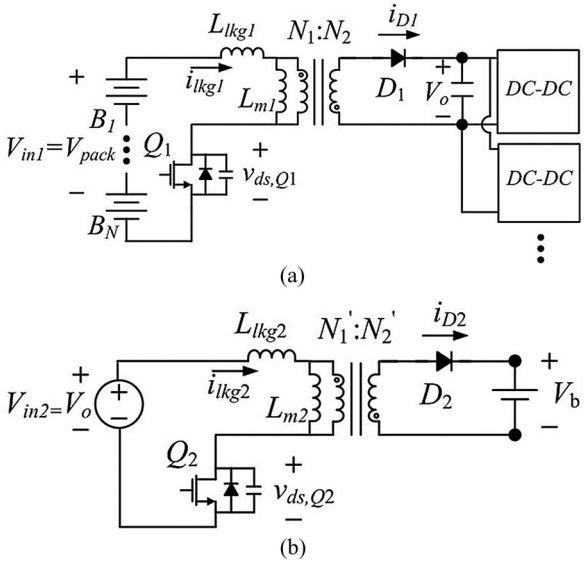

Fig. 9. Power converter for proposed equalizer. (a) First-stage converter. (b) Second-stage converter.

that maximum input power is 12 W at converter efficiency of 80%. Maximum duty ratio for main switch Q_1 is given by

$$D_{\max} = \frac{V_{ds\_\mathrm{nom}} - V_{\mathrm{in}\_\max}}{V_{ds\_\min} + V_{ds\_\mathrm{nom}} - V_{\mathrm{in}\_\max}} \tag{8}$$

where $V_{\mathrm{in}\_\min}$ and $V_{\mathrm{in}\_\max}$ are minimum and maximum voltage for battery pack, respectively. $V_{ds\_\min}$ is minimum voltage stress of main switch. Voltage stress of main switch V_{ds_nom} should guarantee more than 30% margin of maximum drain–source voltage. From the results of (8), we can calculate the transformer inductance. The desired inductance L_m can be obtained by

$$L_m = \frac{(V_{\mathrm{in}\_\min} D_{\max})^2}{2P_{\mathrm{in}} f} \tag{9}$$

where the input power P_{in} is 12 W and switching frequency f is 100 kHz. By using the duty ratio condition and output voltage V_o, the turn ratio of flyback transformer n can be determined as follows:

$$n = \frac{N_1}{N_2} = \frac{V_{\mathrm{in}\_\min} D_{\max}}{(V_o + V_f)(1 - D_{\max})} \tag{10}$$

where V_f is the forward voltage of rectifier diode.

In the second-stage converter, it is required for constant power to battery load without complex control scheme. Hence, the second-stage converter requires that the fixed duty ratio and DCM operation should be guaranteed under minimum battery voltage $V_{b\_\min}$. At this condition, inductance and turn ratio of flyback transformer are obtained by (9) and (10), where $V_{\mathrm{in}\_\min}$ is the output voltage of the first stage and V_o is the minimum battery voltage, $V_{b\_\min}$. As shown in Fig. 10, when the MOSFET switch Q_2 is turned ON during fixed time DT_s, the input power build up with constant value under condition of constant input voltage $V_{\mathrm{in}2}$. Hence, the output current I_{out} can be limited with increasing battery voltage V_b due to constant input power. It makes the boundary condition of maximum charge current for safe converter operation.

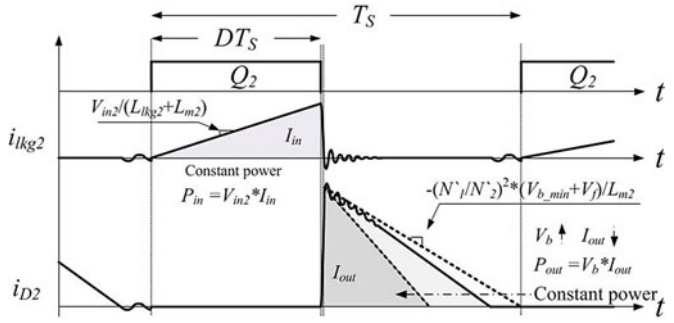

Fig. 10. Current waveform of the second-stage converter.

The cell selection switches are related to the number of divided module unit. If the number of battery module is decreased to minimize the number of modular power converter, voltage stress of selection switches will be increased. Hence, we designed minimum number of module unit under the low voltage stress of cell selection switches. The voltage stress of MOSFET switch has a relationship with the component size and cost. The voltage stress equation for selection switches V_{stress} can be given by

$$V_{\mathrm{stress}} = \left(\frac{N_c}{N_m} - 1\right) V_{b\_\max} \tag{11}$$

where N_c and N_m are the number of battery string and battery module, respectively, as shown in Fig. 2. In (11), $V_{b\_\max}$ indicates maximum voltage of battery cell. In proposed system for 88 lithium-ion battery cells, the number of modules to be designed should be more than eight with a 50% margin of voltage stress.

V. Experimental Results

To show the feasibility of the proposed modularized two-stage equalizer, a prototype for 88 lithium-ion cells was implemented. In practical HEV battery pack, battery system size is the most important factor because the practical size of the battery pack is limited by the number of battery cells. Therefore, the prototype of the proposed work mainly considers the advancement of size reduction compared to a prototype work of conventional method. Fig. 11(a) shows the photograph of the prototype using conventional scheme presented in [19]. As shown in Fig. 11(a), the conventional circuit occupies the single board size of 140 mm × 110 mm; each board takes care of 24 cells without the voltage sensing circuit. For 88 lithium-ion cells, it should be realized with four boards. Furthermore, the conventional circuit has 11 modular dc–dc converters and 88 individual dc–dc converters per each cell. Contrary to the conventional method, the proposed circuit shows the smaller size with lower number of dc–dc converters. Fig. 11(b) shows the photograph of the prototype using proposed scheme. For 88 cells, the proposed equalizer is realized with two boards; thus, each board takes care of 44 cells. With the modularization concept, it has 8 modules, which include the number of 11 cells. The proposed balancing circuit occupies the single board size of 100 mm × 170 mm. In this prototype board, the balancing circuit and the

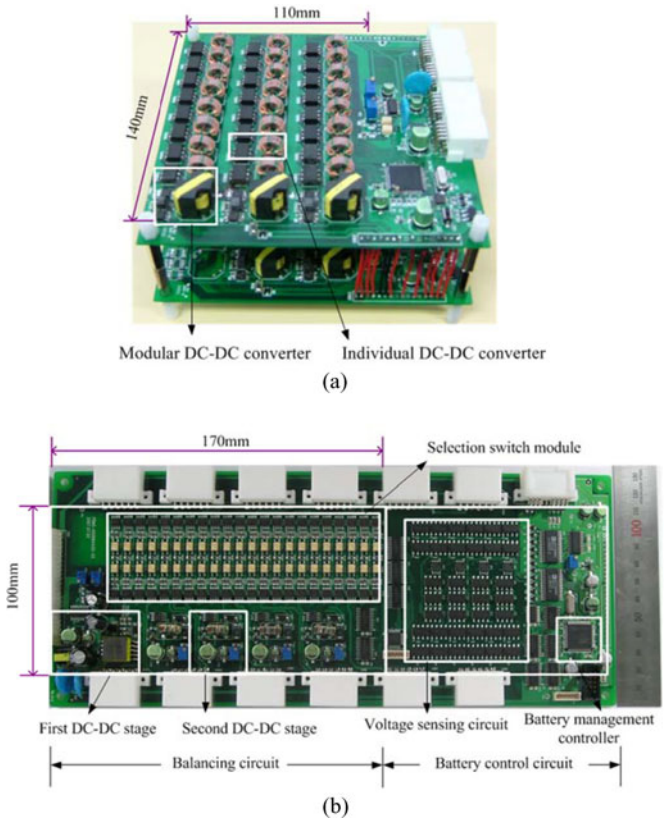

Fig. 11. Photograph of an implemented engineering prototype for 88 lithium-ion battery cell. (a) Conventional equalizer circuit. (b) Proposed equalizer circuit.

TABLE I
PARAMETER OF THE PROTOTYPE

Parameters				*Value*
Balancing circuit	First stage DC-DC converter	MOSFET switch		FQD2N100
		Rectifier diode		10NQ040N
		Trans-former	Core	EP41313
			N_1:N_2	15:1
			L_m	4.1mH
			L_{kg}	125uH
	Second stage DC-DC converter	MOSFET switch		IRF7452
		Rectifier diode		B340AD
		Trans-former	Core	CM102125
			N_1:N_2	28:11
			L_m	56.8uH
			L_{kg}	1.08uH
	Selection switch	P-type		STS3DPF60L
		N-type		SSD2025

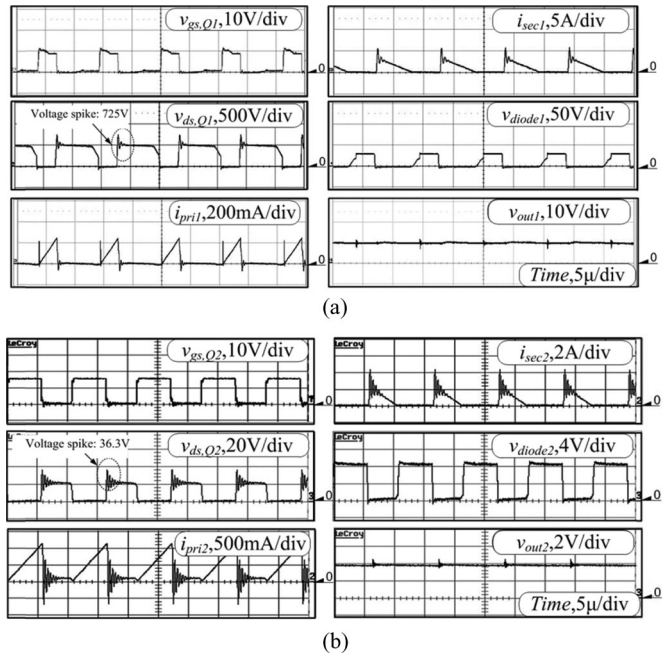

Fig. 12. Experimental waveforms of the two-stage dc–dc converter.(a) First stage. (b) Second stage.

battery control circuit are implemented on the same board, as shown in Fig. 11(b). The proposed circuit uses small number of dc–dc converters with one first-stage dc–dc converter and eight second-stage dc–dc converters. Moreover, we implemented the second-stage converter by applying the low power rating design presented in Section IV, i.e., the output power is designed to be approximately $2\,\mathrm{W} = 4\,\mathrm{V} * 0.5\,\mathrm{A}$. Table I summarizes the parameters of the prototype. One set of experimental parameters presents the first stage of dc–dc converter, and another set shows the second stage of dc–dc converter in each module. The selection switches are also included in Table I.

Fig. 12 shows the experimental waveform of the first- and second-stage dc–dc converter. In the first-stage converter, input voltage is 340 V, which is the stack voltage of 88 battery cells. The output voltage is regulated about 10 V. This voltage of 10 V is similar to the power level of battery control system with a 12 V lead acid battery [19]. The efficiency of the first stage is approximately 82%. The first-stage converter has high voltage stress of the MOSFET switch of about 725 V due to high input voltage of the converter. In the second-stage converter, input voltage is 10 V and the output current is about 0.52 A. The measured efficiency of the second-stage converter is approximately 75% including the conduction loss of the cell selection switches. As shown in Fig. 12(b), the maximum voltage stress at the MOSFET switches does not exceed 37 V, even in the voltage spikes. These results confirm that the second-stage converter has desirable features, such as low voltage stress.

To show the cell balancing performance of the proposed charge equalizer, we conducted an equalization test for 88 cells. The battery control circuit deals with the estimation of the battery SOC for the proposed work. The battery SOC distribution for test environments is summarized in Table II. The test shows two types of balancing test. First test is for two unbalanced cells, $B_{3,3}$ and $B_{6,5}$, which have the equalization procedure at the same time. Since these batteries are in different module for each other, each module can make parallel process of cell balancing. Another test shows the single-cell equalization with large SOC difference between the maximum voltage cell and the undercharged cell. The SOC of the most undercharged cell, $B_{3,2}$ is 35.87%, and the SOC of the maximum voltage cell is 47.7%; thus, SOC difference is approximately 11.8%. In this test, the

TABLE II
SOC DISTRIBUTION OF THE LITHIUM-ION BATTERY CELLS

Parameters		Value [V]	Value [SOC %]
Two cell test	Average voltage cell	3.849V	49.73%
	Undercharged cell $B_{3,3}$ (25th cell)	3.818V	43.96%
	Undercharged cell $B_{6,5}$ (71th cell)	3.810V	42.33%
Single cell test	Average voltage cell	3.830V	46.46%
	Maximum voltage cell	3.837V	47.73%
	Minimum voltage cell (except $B_{3,2}$)	3.829V	46.39%
	Undercharged cell $B_{3,2}$ (target cell)	3.747V	35.87%

BMC control process is as follows: the BMC detects lower SOC cells than a given SOC, and then it drives the equalizer circuit. A given SOC is related to the average SOC of battery pack. In the proposed work, the equalizer is operated at the battery condition of 10% of SOC difference in idle battery pack. The cell balancing test begins when the SOC difference of specific cell shows more than 10% compared to the average SOC. If the undercharged cells are in different module, the modules with the undercharged cell operate at the same time. This equalizer charges the undercharged cell until the programmed equalization time. The equalization time for the battery charge comes from the simulation result, as shown in Fig. 7.

Fig. 13(a) shows the equalization results of two targets cell, 25th cell and 71th cell, within different module for each other. Two undercharged cells begin to charge at the same time. After 28 minutes, the 25th cell terminates the cell balancing. However, the 71th cell keeps operating during 55 min due to the lowest voltage of the 71th cell. From these results, we know that longer equalization time will be taken for the lower SOC level of target cell. Fig. 13(b) shows the balancing performance of single cell with large SOC difference. After the BMC drives the equalizer during 100 min, charge balance is achieved. The SOC difference decrease from the 11.8% to approximately 1%, which value is equivalent to approximately 6 mV. The net equalization current is measured to 0.49 A. It is noted that this experimental results are very similar to the simulation results, as shown in Fig. 7.

Table III shows a comparative study of the proposed equalizer. This study focuses on the implementation problem, balancing performance, and control complexity. Note that the number of batteries is assumed to be 88 cells. In addition, the system size and cost criteria are evaluated by the number of electronic components.

When we compare with centralized control and cell control method, centralized methods have small size, as shown in Table III. However, as mentioned previously, the balancing performance of these methods has a long equalization time. Especially, if the voltage difference between cells is getting smaller and smaller, the balancing performance can be decreased rapidly. To show this problem, we conducted an equalization test for 7

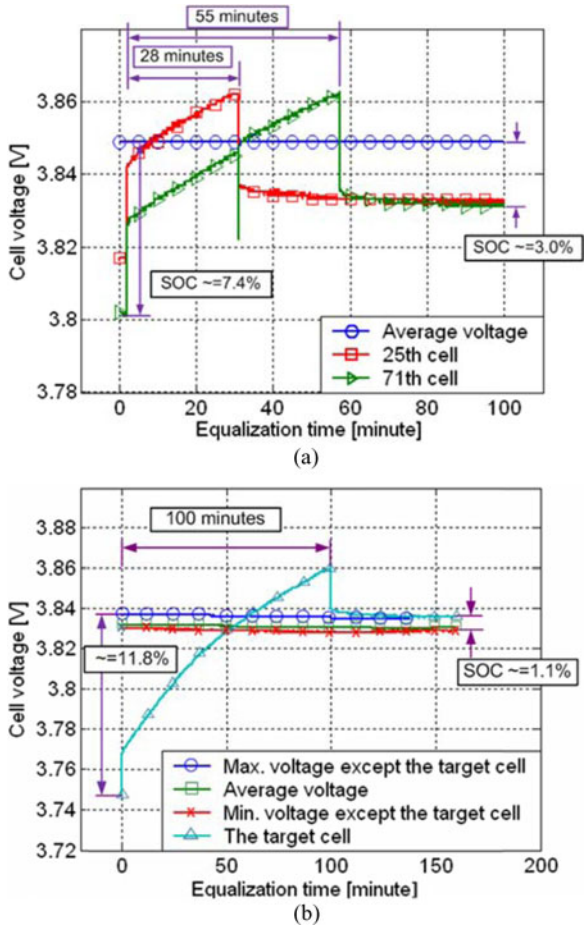

Fig. 13. Results of cell equalization test for 88 lithium-ion battery cells. (a) Two cell balancing test. (b) Single-cell balancing test.

Ah lithium-ion battery. As shown in Fig. 14, cell balancing is not achieved after a long charge equalization time; equalization speed is decreased while the difference of cell voltage is decreased. From these equalization results, the proposed charge equalizer has the advantages of high balancing performance. As shown in Table III, the proposed work also reduces the number of electric component in dc–dc converters because the dedicated dc–dc converter per each cell is replaced by a common dc–dc converter and the cell selection switches. In spite of many selection switches, overall size and cost of the proposed circuit does not increase because these switches can use low power rating MOSFET with small package size. Still, in the proposed circuit, many MOSFET switches for cell selection switches can be weak point of system reliability. If some of the switches show the wrong operation due to the switching fault, whole operation of equalization system can fail in worst case. To minimize this problem, proposed work constructed switch blocks with each module in order to reduce the whole influence when specific batteries become a problem in series circuit. Only through exchanging the modular switch block if there is a switch problem, the whole system can ensure its operation. In order to advance this system, switch block is needed to make an IC method with each module for increasing its reliability.

TABLE III
COMPARATIVE STUDY OF THE PROPOSED EQUALIZER FOR 88 BATTERY CELLS

		Centralized control		*Cell control*				
		Switched cap. [11]	*Multiple windings [12]*	*Proposed*	*buck-boost [16]*	*Intelligent [17]*	*QRZCS [18]*	*Flyback [19]*
DC-DC converter block	Transformer	0	8	9	8	0	0	99
	Diode	0	88	9	88	0	174	88
	Inductor	0	0	0	0	174	261	0
	Capacitor	87	88	9	92	87	87	88
	MOSFET	0	8	9	16	174	174	11
Switch block	MOSFET	176	0	176	88	0	0	88
Balancing performance	Efficiency	**S**	**G**	S	**G**	**E**	**E**	**G**
	Speed	**P**	**P**	**E**	**G**	**S**	**S**	**E**
Control	Simplicity	**E**	**G**	**G**	**P**	**S**	**S**	**G**

E: Excellent, **G**: Good, **S**: Satisfactory, **P**: Poor.

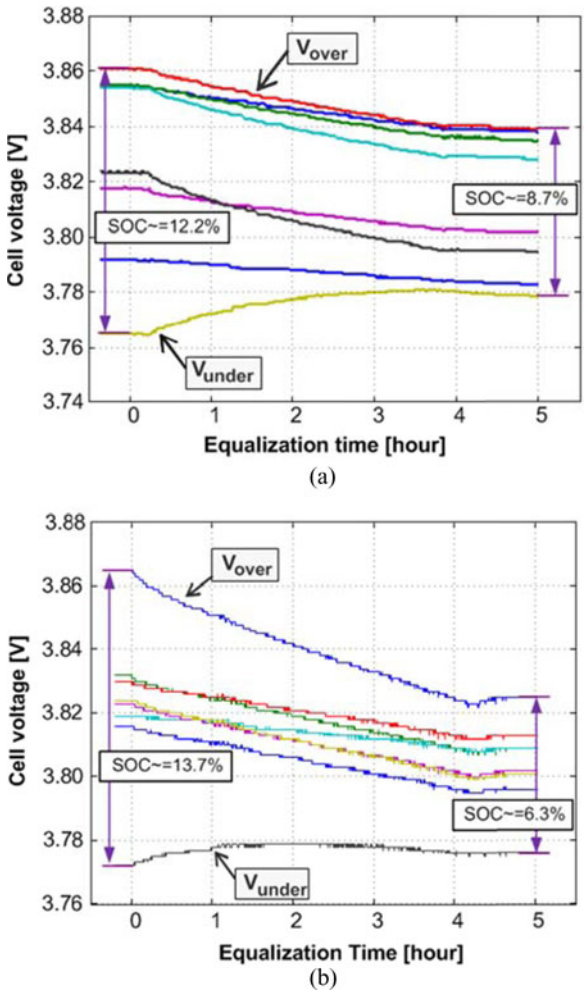

Fig. 14. Comparative results of cell equalization test. (a) Switched capacitor method. (b) Multiple-winding method.

From this comparative study, we conclude that the proposed equalizer can be used for an equalization system that requires a good cell balancing performance, simple control scheme, and small size with lower cost.

VI. CONCLUSION

In this paper, the modularized two-stage charge equalizer with cell selection switches was proposed. The proposed method was specifically implemented for a very long battery string of 88 cells; the type of string that is used for an HEV application. The design consideration, the comparison study with previous contributions, and the cell balancing performance for 88 cells have been also presented. The proposed scheme shows the low voltage stress of the electronic devices and easy implementation by using the modularized two-stage dc–dc converter. In addition, with sharing connection of dc–dc converter and cell selection switches, the proposed equalizer solves the size problem of equalizer implementation for a large number of battery cells. Experimental results on 88 lithium-ion battery systems demonstrate that the proposed circuit has outstanding equalization performance and small implementation size. Therefore, the proposed equalizer can be widely used for a high stack of lithium-ion battery cells in an HEV.

REFERENCES

[1] C. C. Chan, "The state of the art of electric, hybrid, and fuel cell vehicles," in *Proc. IEEE*, Apr., 2007, vol. 95, pp. 704–718.
[2] I. Aharon and A. Kuperman, "Topological overview of powertrains of battery-powered vehicles with range extenders," *IEEE Trans. Power Electron.*, vol. 26, no. 3, pp. 868–876, Mar. 2011.
[3] A. Emadi, Y. J. Lee, and K. Rajashekara, "Power electronics and motor drives in electric, hybrid electric, and plug-in hybrid electric vehicles," *IEEE Trans. Ind. Electron.*, vol. 55, no. 6, pp. 2237–2245, Jun. 2008.
[4] A. Emadi, S. Williamson, and A. Khaligh, "Power electronics intensive solutions for advanced electric, hybrid electric, and fuel cell vehicular power systems," *IEEE Trans. Power Electron.*, vol. 21, no. 3, pp. 567–577, May 2006.

[5] S. M. Lukic, J. Cao, R. C. Bansal, F. Rodriguez, and A. Emadi, "Energy storage system for automotive applications," *IEEE Trans. Ind. Electron.*, vol. 55, no. 6, pp. 2258–2267, Jun. 2008.
[6] M. Bradgard, N. Soltau, S. Thomas, and R. W. De Doncker, "The balance of renewable sources and user demands in grids: Power electronics for modular battery energy storage system," *IEEE Trans. Power Electron.*, vol. 25, no. 12, pp. 3049–3056, Dec. 2010.
[7] A. Affanni, A. Bellini, G. Franceschini, P. Guglielmi, and C. Tassoni, "Battery choice and management for new-generation electric vehicles," *IEEE Trans. Ind. Electron.*, vol. 52, no. 5, pp. 1343–1349, Oct. 2005.
[8] N. Takeda, S. Imai, Y. Horii, and H. Yoshida, "Development of high-performance lithium-ion batteries for hybrid electric vehicles," *Mitsubishi Motors Tech. Review*, pp. 68–72, 2003.
[9] B. T. Kuhn, G. E. Pitel, and P. T. Krein, "Electrical properties and equalization of lithium-ion cells in automotive applications," in *Proc. IEEE Vehicle Power Propulsion Conf.*, 2005, pp. 55–59.
[10] C. Pascual and P. T. Krein, "Switched capacitor system for automatic series battery equalization," in *Proc. IEEE Appl. Power Electron. Conf. Exp.*, 1997, pp. 848–854.
[11] A. Baughman and M. Ferdowsi, "Double-tiered capacitive shuttling method for balancing series-connected batteries," in *Proc. IEEE Vehicle Power Propulsion Conf.*, 2005, pp. 50–54.
[12] N. H. Kutkut, H. L. N. Wiegman, D. M. Divan, and D. W. Novotny, "Design considerations for charge equalization of an electric vehicle battery system," *IEEE Trans. Ind. Appl.*, vol. 35, no. 1, pp. 28–35, Feb. 1999.
[13] D. M. Divan, N. H. Kutkut, D. W. Novotny, and H. L. Wiegman, "Battery charging using a transformer with a single primary winding and plural secondary windings," U.S. Patent 5 659 237, August 1997.
[14] B. Lindemark, "Individual cell voltage equalizers (ICE) for reliable battery performance," in *Proc. IEEE Int. Telecommun. Energy Conf.*, 1991, pp. 196–201.
[15] Y. Xi and P. K. Jain, "A forward converter topology with independently and precisely regulated multiple outputs," *IEEE Trans. Power Electron.*, vol. 18, no. 2, pp. 648–658, Mar. 2003.
[16] M. Tang and T. Stuart, "Selective buck-boost equalizer for series battery packs," *IEEE Trans. Aerosp. Electron. Syst.*, vol. 36, no. 1, pp. 201–211, Jan. 2000.
[17] Y.-S. Lee and M.-W. Cheng, "Intelligent control battery equalization for series connected lithium-ion battery strings," *IEEE Trans. Ind. Electron.*, vol. 52, no. 5, pp. 1297–1307, Oct. 2005.
[18] Y.-S. Lee and G.-T. Cheng, "Quasi-resonant zero-current-switching bidirectional converter for battery equalization applications," *IEEE Trans. Power Electron.*, vol. 21, no. 5, pp. 1213–1224, Sep. 2006.
[19] H.-S. Park, C.-E. Kim, C.-H. Kim, G.-W. Moon, and J.-H. Lee, "A modularized charge equalizer for an HEV lithium-ion battery string," *IEEE Trans. Ind. Electron.*, vol. 56, no. 5, pp. 1464–1476, May 2009.
[20] C.-H. Kim, H.-S. Park, C.-E. Kim, G.-W. Moon, and J.-H. Lee, "Individual charge equalization converter with parallel primary winding of transformer for series connected lithium-ion battery strings in an HEV," *J. Power Electron.*, vol. 9, pp. 472–480, May 2009.
[21] P. A. Cassani and S. S. Williamson, "Design, testing, and validation of a simplified control scheme for a novel plug-in hybrid electric vehicle battery cell equalizer," *IEEE Trans. Ind. Electron.*, vol. 57, no. 2, pp. 3956–3962, Dec. 2010.
[22] S. W. Moore and P. J. Schneider, "A review of cell equalization methods for lithium ion and lithium polymer battery systems," *SAE Tech. Paper Series*, pp. 1–5, Mar. 2001.
[23] L. Palma and P. N. Enjeti, "A modular fuel cell, modular DC-DC converter concept for high performance and enhanced reliability," *IEEE Trans. Power Electron.*, vol. 24, no. 6, pp. 1437–1443, Jun. 2009.
[24] H.-S. Park, C.-H. Kim, K.-B Park, G.-W. Moon, and J.-H. Lee, "Design of a charge equalizer based on battery modularization," *IEEE Trans. Veh. Technol.*, vol. 58, no. 7, pp. 3216–3223, Sep. 2009.
[25] L. Maharjan, S. Inoue, H. Akagi, and J. Asakura, "State-of-charge-balancing control of a battery energy storage system based on a cascade PWM converter," *IEEE Trans. Power Electron.*, vol. 24, no. 6, pp. 1628–1636, Jun. 2009.
[26] L. Maharjan, S. Inoue, T. Yamagishi, H. Akagi, and J. Asakura, "Fault-tolerant operation of a battery-energy-storage system based on a multilevel cascade PWM converter with star configuration," *IEEE Trans. Power Electron.*, vol. 25, no. 9, pp. 2386–2396, Sep. 2010.
[27] I.-S. Kim, "A technique for estimating the state of health of lithium batteries through a dual-sliding-mode observer," *IEEE Trans. Power Electron.*, vol. 25, no. 4, pp. 1013–1022, Apr. 2010.

Chol-Ho Kim (S'07) was born in Iksan, Korea, in 1982. He received the B.S. and M.S. degrees in electrical engineering from the Korea Advanced Institute of Science and Technology, Daejeon, Korea, in 2006 and 2008, respectively, where he is currently working toward Ph. D. degree.

His current research interests include the design and control of battery management system, charge equalization converter, and low-voltage high-current dc/dc converters.

Mr. Kim is a member of the Korea Institute of Power Electronics.

Moon-Young Kim (S'10) was born in Korea, in 1982. He received the B.S. degree from Kyung-Pook National University, Deagu, Korea, in 2008, and the M.S. degree in the electrical engineering from the Korea Advanced Institute of Science and Technology, Daejeon, Korea, in 2010, where he is currently working toward the Ph.D. degree.

His main research interests include dc/dc converter, cell balancing circuit, and battery management system.

Mr. Kim is a member of the Korean Institute of Power Electronics.

Hong-Sun Park (S'01–A'09) was born in Korea, in 1974. He received the B.S. degree in electronic engineering from Sogang University, Seoul, Korea, in 2000, and the M.S. and Ph.D. degrees in electrical engineering from the Korea Advanced Institute of Science and Technology, Daejeon, Korea, in 2003 and 2009, respectively.

He is currently a Senior Engineer with Samsung Electro-Mechanics. His research interests include the design and control of a dc–dc converter, hybrid electric vehicle (HEV) battery management system, HEV battery equalizer, and LED lighting power supply.

Gun-Woo Moon (S'92–M'00) received the M.S. and Ph.D. degrees in electrical engineering from the Korea Advanced Institute of Science and Technology (KAIST), Daejeon, Korea, in 1992 and 1996, respectively.

He is currently a Professor in the Department of Electrical Engineering, KAIST. His research interests include modeling, design, and control of power converters, soft-switching power converters, resonant inverters, distributed power systems, power-factor correction, electric drive systems, driver circuits of plasma display panels, and flexible ac transmission systems.

Dr. Moon is a member of the Korean Institute of Power Electronics, Korean Institute of Electrical Engineers, Korea Institute of Telematics and Electronics, Korea Institute of Illumination Electronics and Industrial Equipment, and Society for Information Display.